



TITLE:

# On the Explosion Spectra of Hg, Cu, and Fe

AUTHOR(S):

Hori, Takeo

---

CITATION:

Hori, Takeo. On the Explosion Spectra of Hg, Cu, and Fe. Memoirs of the College of Science, Kyoto Imperial University. Series A 1926, 9(6): 379-403

ISSUE DATE:

1926-07-01

URL:

<http://hdl.handle.net/2433/256766>

RIGHT:

# On the Explosion Spectra of Hg, Cu, and Fe.

By

**Takeo Hori.**

(Received October 2, 1925)

---

After the method of Anderson, the present writer has investigated the absorption spectra produced by the explosion of a fine metallic wire in a confined space. The rectified current from the transformer, whose primary circuit operates on a 220-volt A. C. power line through a resistance and whose secondary furnishes 1 k W 2,5000 volts (max.), charges a condenser of capacity about 0.3 micro-farad, and the discharge is brought about automatically through an adjustable spark gap and a fine wire.

As will easily be seen, the concentration of the energy input in the wire is the greater, the finer and shorter the wire is. Moreover, the space in which the explosion takes place, should be made as narrow as possible, so that we may obtain good absorption spectra.

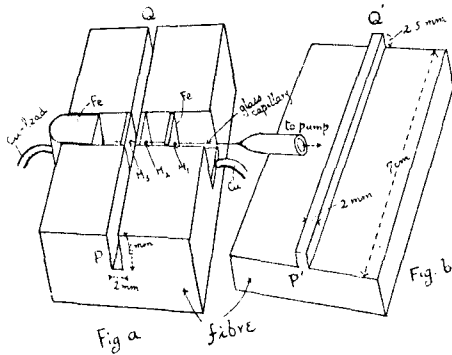
By varying the length of the spark gap, the voltage at which the explosion occurs, can be regulated at will, so that the stage, in which a line comes out reversed, may be determined by such regulation.

The following gives the experimental arrangement and the results for mercury, copper, and iron.

## § 1. Mercury.

The mercury filament to be exploded was made by sucking mercury into a fine glass capillary. The process was as follows.

The two small cavities A and B (Fig. a) were filled with mercury, and into these was inserted a very slender capillary, the prolongation of the ordinary glass tube, through small holes  $H_1$ ,  $H_2$ , and  $H_3$ . The tube



was connected to a rotary pump and as the sucking of the mercury at A was going on, the capillary was suddenly snapped down at C by a small knife edge. Both pools of mercury were thus electrically connected through a fine tube.

This bridge of mercury filament was exploded at the center of a cut PQ made at right angles to the filament in a fibrous block. Fig. b shows the lid, with which to cover the cut during the explosion, the projection P' Q' fitting in the upper portion of the cut. On the lid was further put a lead block.

The spectra were taken on the end-on direction by a constant-deviation-prism spectrograph on one side and by a small quartz spectrograph on the other. Five or six successive explosions were necessary to give sufficient density on the plate.

(a) Explosions in the open air:—

with the present condenser and the maximum voltages attainable, the spectrum showed fairly continuous background especially in the ultra-violet region. The following lines appeared as absorption lines (Figs. A and C.)

Table I.

$\lambda$	notation	$\lambda$	notation
2537	1s-2p <sub>2</sub>	3132	2p <sub>2</sub> -3d <sub>3</sub>
2652	2p <sub>2</sub> -4d <sub>2</sub>	3650	2p <sub>1</sub> -3d <sub>1</sub>
2654	2p <sub>2</sub> -4d <sub>3</sub>	3655	2p <sub>1</sub> -3d <sub>2</sub>
2894	2p <sub>2</sub> -3s	3663	2p <sub>1</sub> -3d <sub>3</sub>
2967	2p <sub>3</sub> -3d <sub>3</sub>	4047	2p <sub>3</sub> -2s
3022	2p <sub>1</sub> -4d <sub>1</sub>	4358	2p <sub>2</sub> -2s
3126	2p <sub>2</sub> -3d <sub>2</sub>	5461	2p <sub>1</sub> -2s

As the spark length was varied from minimum to maximum a line changed from the stage of emission to that of self-reversal and then to a normal absorption. Whatever the true cause of continuous radiation may be, there is no doubt but that the Stark broadening of some or all of the

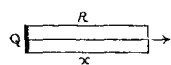
lines makes an important contribution to the development of the continuous spectrum observed at final stages.

As regards the order in which the reversal of one line appeared after another, the mere fact can be given at present that the lines of the diffuse series can be reversed at an earlier stage than those of the sharp series. But it is easy to see\* that the reversal on the photographic plate is the superposed effect of so many a factor that we cannot give any simple physical interpretation for the observed absorption stages.

(b) Explosions under reduced pressure;—

Putting the above described arrangement under a metallic jar provided with quartz windows and connected to a pump, the explosion was made

Note 1 \* Suppose for simplicity's sake that the continuous radiation from a source Q passes through an absorbing layer R of length  $x$ , throughout which the condition of the vapour is constant. The intensity of radiation from Q and R together, as viewed from a distant point on the axis of R, is given by



$$J = Ie^{-Ax} + \frac{E}{A} (1 - e^{-Ax}),$$

where  $I$  represents the intensity of radiation from the source,  $E dx$  the intensity radiated from a layer of thickness  $dx$  in  $R$ , and  $A$  the absorption coefficient of the layer. The condition for reversal is that

$$I - J > 0, \\ \text{i. e. } (I - E/A) (1 - e^{-Ax}) > 0 \dots\dots\dots(1), \\ \text{or, since } 1 > e^{-Ax}, I > E/A \dots\dots\dots(2).$$

Here the quantity  $A$  is dependent upon two factors: one, the relative concentration of the atoms in a state capable of the absorption; and the other, the absorbing power of the state itself or "the atomic absorption coefficient." The latter may be deemed the characteristic constant of the state. Hence, favorable conditions for a line to reverse would be

- (i) that the intensity of the back-ground in the vicinity of the line should be sufficiently great;
- (ii) that an absorbing layer of sufficient length should give a maximum concentration of the atoms in that state from which they make transit to the upper by way of absorption of the line (—The dependence of the concentration upon temperature and pressure will be described in Note 2.—); and
- (iii) that in the layer there should be a minimum amount of emission of the line in question.

Thus the order of reversal that came out on the photographic plate allows us not to compare the quantity  $A$  but the ratio  $E/A$  for each line, and that provided the back-ground intensity remains constant. Much less, we are not measuring the atomic absorption coefficient. If we also take the circumstances into account that we are observing on the plate the superposition of every instantaneous effect during the explosion, and, furthermore, that the sharpness of the line and the resolving power of the instrument as well as of the photographic plate are the factors of practical importance in determining whether we can observe the absorption or not, we find it entitled to little weight to seek for any simple physical interpretation for the observed facts.

under reduced pressure (ca. 5 mm.). The development of the continuous back-ground was much more satisfactory than in the preceding case and the easiness of the occurrence of absorption lines seemed rather peculiar.\*\* Besides the lines given in Table I, the following three lines appeared as distinct absorption lines. (cf. Figs. A, (b); C, (c))

Table II.

$\lambda$ 3342	(2P <sub>1</sub> - 3S)
$\lambda$ 5770	(2P - 3D <sub>2</sub> )
$\lambda$ 5791	(2P - 3D)

(C) Remarks:—

(i) It is remarkable that in a certain case, when by chance the machine oil (—used as a temporary cementing material between the metallic cover and the stand (made of ebonite) through which the leading wires were introduced—) spoiled the wall of the exploding space, the Swan spectrum manifested itself as an absorption band (cf. Fig. C (a)), which

Note 2. \*\* The following note may give a somewhat distinct idea about what is taking place in the actual process. The space at which the explosion occurs is so confined that a continuous spectrum is produced owing to the high pressure momentarily caused by the explosion. Its intensity  $I$  will therefore be none-the-less great because it is not exploded under an atmospheric pressure. (Compare Figs. A, (a) and (b); Figs. B, (b) and (c).) The vapour which forms the absorbing layer is very much prolonged in length  $x$ , along which the pressure varies from minimum to maximum.

The emission per unit length  $E$  of the absorbing layer will decrease, as the result of its prolongation, while the absorption coefficient  $A$  never diminishes in the same ratio as  $E$ , for the average life of an excited atom may be supposed to increase under reduced pressures and the longer maintenance of the concentration of the atoms in excited states would result therefrom. Thus the equation (1) of Note I suggests the easiness of reversal in the present case.

In support of the latter supposition are given the following considerations:

- (i) When the explosion occurs under reduced pressures, the external work done by the expansion of the excited vapour may be so diminished, that the temperature lowering of the vapour would be much less than in the case of open-air explosions. The longer maintenance of a number of excited atoms would therefore result from the high speed collisions between atoms and electrons.
- (ii) If the suggestion is true that the transition (of either the first or the second kind) of an atom from the upper state to the lower is caused by the disturbing influence from neighbouring atoms or electrons, an influence which comes into play especially when they approach closely to each other, we can increase the duration of life of an excited atom by reducing the pressure, for then the mean time interval, during which it can make free flight, would be lengthened. The longer duration of life renders the absorbing power  $A$  larger.
- (iii) The above considerations seem to be supported from the thermodynamical point of view by Saha's theory.

fact, so far as I am aware, is as yet unobserved in the laboratory.

(ii) The line 2537 showed in the explosion in vacuo an absorption abnormally extended to the less refrangible side. See Fig. A (b), in which it also manifests a double reversal.

(iii) Among the lines of impurities that came out reversed, the following may be worthy of note.

Table III.

---

Na: 6161, 6154	(2p <sub>1</sub> -3d, 2p <sub>2</sub> -3d)	
		5688, 5683 (2p <sub>1</sub> -4s, 2p <sub>2</sub> -4s) (cf. Fig. C, (b) (c))
Ca: 6500 } 6494 }	(Unclassified pair Δν = 13.88)	
6472 } 6463 }	( " " Δν = 21.72)	
6456 } 6450 }	( " " Δν = 13.90)	
6162 } 6122 }	(2p <sub>1</sub> -2s) (2p <sub>2</sub> -2s)	
6103 }	(2p <sub>3</sub> -2s)	
5603 } 5599 }	(Δν = 13.85)	} Triplet (3d <sub>z</sub> -md <sub>z</sub> ) (Götze, Ann. d. Phys. 66, 285, 1921)
5601 }	(Δν = 21.76)	
5595 }	(Δν = 13.92)	
5589 }	(Δν = 21.70)	
5582 }		
5270 } 5264 }	(Δν = 21.76) (Δν = 13.93)	} Triplet (3d <sub>z</sub> -3p <sub>z</sub> ) (Popow, Ann. d. Phys. 45, 147, 1914)
5260 }		
5266 } 5262 }	(Δν = 13.92)	
4457 }	(2p <sub>1</sub> -4d <sub>3</sub> )	
4456 }	(2p <sub>1</sub> -4d <sub>2</sub> )	
4455 }	(2p <sub>1</sub> -4d <sub>1</sub> )	
4436 }	(2p <sub>2</sub> -4d <sub>3</sub> )	
4435 }	(2p <sub>2</sub> -4d <sub>2</sub> )	

4425	( $2p_3 - 4d_3$ )		
4319	} ( $\Delta v = 105.85$ )	} Triplet ( $2p - 3p$ ) (Götze, l.c.p. 291)	
4299			} ( $\Delta v = 52.20$ )
4289			
4303	} ( $\Delta v = 105.87$ )		
4283			
4227	( $1s - 2p$ )		
3968	( $2\mathfrak{F}_2 - 2\mathfrak{C}$ )		
3934	( $2\mathfrak{F} - 2\mathfrak{C}$ )		

(cf. Figs. A, (a) (b); C, (b) (c))

Al: Lines of I.S.S. & II.S.S. were reversed (Fig. A, (a) (b))

Si:  $\lambda\lambda$  2882, 2631, 2529, 2524, 2519, 2516, 2514, 2507, 2452, 2435—

All of these belong to arc lines (Figs. A and B).

Fe: Characteristic iron lines appeared in the spectrum. See §3.

### § 3. Copper.

A fine copper-wire (No. 45) was placed between two copper terminals, 2 mm. apart, connection being made by squeezing the end of the wire between two parallel plates by means of a screw. The development of the continuous back-ground was much poorer than in the preceding case and the reversal was observed only for the lines of the characteristic doublet ( $\lambda\lambda$  3274, 3248) and for those in the ultra-violet end of the spectrum ( $< \lambda$  2550).

Good results, however, were obtained when the copper-terminals were replaced by two pools of mercury, as was the case with the explosion of a mercury filament, and a hole was bored along the length of the wire to be exploded, which was bridged over the pools. In the spectrum was developed a very satisfactory back-ground; this might have come mainly from the mercury vapour excited at the same time with the explosion.

Almost all the arc lines were now seen reversed, containing those lines, that have hitherto been listed as reversed neither in the arc nor in spark under water. They are tabulated in the following list. (See Figs. 1, 2, 3.) (Lines which are close together and which were not resolved by the small spectrograph are bracketed together.)

Table IV.

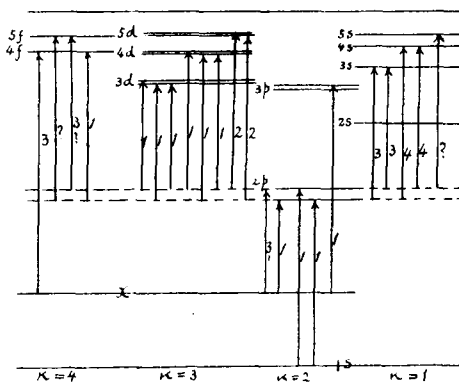
$\lambda$	Absorption stages	Series classification and remarks	$\lambda$	Absorption stages	Series classification and remarks
6162-47	2	Band	4416	3	
6046-60	2	Band	4378	3	
5782	1	$x-2p_2$	4275	3	
5700	3	$x-2p_1$	4260	3	
5555	6		4249	3	
5536	5		4242	6	
5432	5		4178	3	
5409	5		4063	1	$2p_1-4d_1$ $2p_1-4d_1$
5392	5		4056	1	$2p_2-4f$
5355	5		4023	1?	$2p_2-4d_2$
5353			4	$2p_1-4s$	
5293	4		3862	4	$2p_2-4s$
5251	5		3825	4	$2p_2-4s$
5220	1	$2p_1-3d_2$	3688	2	$2p_1-5d_2$
5218		$2p_1-3d_1$	3654	2	$2p_2-5d_2$
5153	1	$2p_2-3d_2$	3652		$2p_2-5f$
5106	1	Diffuse broadening occurs in the final stages	3602	3	$2p_1-5s$
			3599		
5076	5		3533	3	
5035	5		3530		
5017	5		3512	3	$2p_1-5f$
4866	5		(3500-3400)		Many lines in this range are faintly reversed.
4794	5		3381	5	
4705	5		3365	5	
4698	5		3338	4	
4675	3		3308	2	
4651	3		3291	2	
4643	6		3274	1	$1s-2p_2$
4587	3		3248	1	$1s-2p_1$
4540	3		3208	4	
4531	3	$2p_1-3s$	3194	3	
4513	3		3176	5	
4510			3170	5	
4508			3146	3	
4481	3	$2p_2-3s$	3142	2	
			3140		



$\lambda$	Absorption stages	Series classification and remarks	$\lambda$	Absorption stages	Series classification and remarks
3128	?	coincident with Hg 3126	2824	1	x-3p <sub>1</sub>
3126			2766	1	
3116	2	2618	1		
3109	2	2492	1		
3100	2	2442	1		
3094	2	2407	1		
3074	6	2393	1		
3063	3	2370	3	x-4f	
3036	2	2320	1		
3011	2	2303	1		
2997	3	2294	1		
2961	1	2263	1		
2883	3	2260	1		
2859	5				

The number given in the second column indicates the order in which the line came out reversed when the voltage was varied. The fact may be pointed out that the lines belonging to the diffuse series are more easily reversed than those belonging to the sharp series. (This seemed also to be the case with mercury—§I.) See Fig. c, the diagrammatical representation of the absorption of Cu-atom.

Fig. c.



Energy diagram of Cu-atom. Absorption is represented by arrows, subindicated numbers showing the absorption stages. Number given on the right of each horizontal line is the term of the level.

The series classification for copper has hitherto been established only for relatively few lines as indicated above, the tracing of series or the establishment of any physical inter-relationship for other lines being urgently looked for.

As for the absorption of these un-classified lines, it may merely be noticed that there exists a general tendency that lines of shorter wave-lengths are reversed in earlier stages than those of longer wave-lengths.

This might possibly be due to the earlier development of an

intense back-ground in the ultra-violet region.

It is quite interesting to note that most of the lines in the visible region show reversal with emission edges on the red side of them. (cf. Fig. 1, stages 3, 4.) The same is also observed in the case of iron lines. (Fig. 6) The question whether this is due to the Doppler effect or to the peculiar broadening or shifting of the original lines is worthy of further investigation.

### § 2. Iron.

The absorption spectrum of iron was studied in the same manner as copper. The wire used was of No. 36 and gave good results, which are shown in the table below. The series notation is due to Laporte\* and the wave-lengths are taken from Kayser's "Hand-buch" Bd. VII. (cf. Figs. 4, 5, 6.) Absorption stages and the temperature classes due to King are given in the second and the third column respectively.

Table V.

$\lambda$	Absorption stages	Temperature classes	Notation	$\lambda$	Absorption stages	Temperature classes	Notation
5615.663	6	IV	$f_5^1 - d_4^2$	5364.859	?	V	—
5602.965	6	IV	$f_1^1 - d_1^2$	5341.931	6	II	$\bar{F}_2^1 - \bar{D}_2^0$
5586.772	6	IV	$f_4^1 - d_3^1$	5339.949		V	$\bar{d}_2^1 - d_3^2$
5576.106	6	IV	$f_1^1 - d_0^2$	5328.044		I	$\bar{f}_4^1 - \bar{d}_3^1$
5772.857		IV	$f_3^1 - d_2^2$	5324.196	4 5	IV	$\bar{d}_4^1 - d_4^2$
5569.631	6	IV	$f_2^1 - d_1^2$	5302.315	5	V	$\bar{d}_1^1 - d_2^2$
5455.617	5	IB	$\bar{f}_1^1 - \bar{d}_1^1$	5283.634	5	IV	$\bar{d}_3^1 - d_3^2$
5446.922	5	IB	$\bar{f}_2^1 - \bar{d}_2^1$	5281.805		II	$\pi_2 - \delta_3$
5434.527	5	IB	$\bar{f}_1^1 - \bar{d}_0^1$	5270.357	4	II	$\bar{F}_2^1 - \bar{D}_1^0$
5429.701	5	IB	$\bar{f}_3^1 - \bar{d}_3^1$	5269.538		IB	$\bar{f}_5^1 - \bar{d}_4^1$
5424.057	6	V	—	5232.954		5	III
5415.189	6	V	—	5227.187	5	II	$\bar{F}_3^1 - \bar{D}_2^0$
5405.780	5	IB	$f_2^1 - \bar{d}_1^1$	5226.876		IV	$\pi_2 - \delta_2$
5397.135	5	IB	$\bar{f}_4^1 - \bar{d}_4^1$	5216.277	6	II	$\bar{F}_2^1 - F_2^0$
5383.366	6	V	—	5192.364	5	IV	$\pi_3 - \delta_3$
5371.496	5	IB	$\bar{f}_3^1 - \bar{d}_2^1$	5191.475		IV	$\pi_2 - \delta_1$
5369.960	?	V	—	5171.601	6	II	$\bar{F}_3^1 - F_4^0$
5367.455	?	V	—	5167.492	5	II	$\bar{F}_4^1 - \bar{D}_3^0$

\* Zs. f. phys., 23, 135 (1924); 26, 1 (1924).

$\lambda$	Absorption stages	Temperature classes	Notation	$\lambda$	Absorption stages	Temperature classes	Notation
5151.916	6	IB	—	4891.510	4	III	$\varphi_4 - \delta_3$
5150.845		IB	—	4890.770		III	$\varphi_2 - \delta_2$
5139.481	6	IV	$\pi_4 - \delta_4$	4859.757	5	III	$\varphi_2 - \delta_1$
5139.269		IV	$\pi_3 - \delta_2$	4736.788	6	II	$\bar{d}_4^1 - \bar{f}_5^2$
5133.676	6	V	—	4707.287	6	IV	$\bar{d}_3^1 - \bar{f}_4^2$
5123.727	6	IB	$f_1^1 - f_1^1$	4691.416	7	IV	—
5110.414	6	IB	$d_4^1 - \delta_4$	4678.856	7	V	—
5107.645		II	$F_3^1 - F_2^0$	4668.153	6	IV	$d_2^1 - f_3^2$
5107.454	6	IB	$\bar{F}_2^1 - f_2^1$	4654.637	6	IV	$\bar{d}_4^1 - f_3^2$
5098.706		IV	$\bar{p}_3 - p_2^2$	4556.128	6	V	—
5083.344	6	IB	$f_3^1 - f_3^1$	4528.624	6	II	$\bar{p}_3 - \bar{d}_4^3$
5079.742		IB	$f_2^1 - f_1^1$	4525.154	6	IV	—
5079.228	6	IV	$\bar{p}_2 - p_1^2$	4494.571	6	II	$\bar{p}_2 - \bar{d}_3^3$
5074.750		V	—	4489.744	6	IA	$d_0^1 - \varphi_1$
5068.784	6	V	$\pi_4 - \delta_3$	4482.262	6	I	$\bar{p}_1 - \bar{d}_2^3$
5065.016		V	—	4482.176		I	$d_1^1 - \varphi_2$
5051.643	6	IB	$f_4^1 - f_4^1$	4476.023	6	III	—
5049.830		III	—	4469.390	6	IV	—
5041.763	6	III	$F_4^1 - F_3^0$	4466.557	6	II	$d_1^1 - \varphi_0$
5041.073		IB	$\bar{F}_3^1 - f_2^1$	4461.658	6	I	$d_2^1 - \varphi_3$
5027.144	6	—	—	4459.128	6	III	$\bar{p}_3 - \bar{d}_3^3$
5022.255		V	—	4454.387	6	III	—
5014.960	6	V	—	4447.727	6	II	$\bar{p}_1 - \bar{d}_1^3$
5012.073		IB	$f_5^1 - f_5^1$	4442.349	6	III	$\bar{p}_2 - \bar{d}_2^3$
5006.134	6	III	$\varphi_5 - \delta_5$	4435.154	5?	IA	$d_2^1 - \varphi_1$
5005.792		V	—	4430.622	6?	II	$\bar{p}_1 - \bar{d}_0^3$
5001.881	6	V	—	4427.313	5?	I	$\bar{d}_3^1 - \varphi_4$
4985.562		V	$\varphi_3 - \delta_4$	4415.127	4	II	$\bar{F}_2^1 - \bar{g}_3^1$
4985.267	6	V	—	4408.420	6	III	$\bar{p}_3 - \bar{d}_2^3$
4983.858		V	—	4407.716		III	$\bar{p}_2 - \bar{d}_1^3$
4982.524	4	V	—	4404.752	3	II	$\bar{F}_3^1 - \bar{g}_4^1$
4957.612		III	$\varphi_6 - \delta_5$	4383.548	2	II	$\bar{F}_4^1 - \bar{g}_5^1$
4957.311	4	III	$\varphi_4 - \delta_4$	4375.934	3	I-II	$d_4^1 - \varphi_5$
4938.828		IV	$\varphi_2 - \delta_3$	4352.740	5	III	$\bar{p}_1 - s_2$
4920.521	4	III	$\varphi_5 - \delta_4$	4337.052	5	II	$F_3^1 - \bar{g}_3^1$
4919.008		III	$\varphi_3 - \delta_3$	4325.770	3	II	$F_2^1 - C_3^1$
4903.325	5	III	$\varphi_1 - \delta_2$	4315.090	6	III	$\bar{p}_2 - s_2$

$\lambda$	Absorption stages	Temperature classes	Notation	$\lambda$	Absorption stages	Temperature classes	Notation
4307.910	3	II	$\bar{F}_3^1 - \bar{G}_4^1$	4154.819		IV	—
4299.254	4	III	$\bar{\delta}_4 - \bar{\delta}_5$	4154.504	4	III	—
4294.132	5	II	$\bar{F}_4^1 - \bar{g}_4^1$	4153.902		IV	—
4282.408	5	III	$\bar{P}_3 - \bar{s}_2$	4147.675	6	III	$\bar{F}_4^1 - \bar{G}_3^1$
4271.764	2-3	II	$\bar{F}_4^1 - \bar{G}_5^1$	4143.874	3	I	$\bar{F}_3^1 - \bar{F}_4^1$
4271.171		III	$\bar{\delta}_3 - \bar{\delta}_4$	4137.002	5	IV	—
4260.489	3	III	$\bar{\delta}_5 - \bar{\delta}_5$	4134.684	5	IV	—
4250.791	3	II	$\bar{F}_3^1 - \bar{G}_3^1$	4132.064	3	II	$\bar{F}_2^1 - \bar{F}_3^1$
4250.134		III	$\bar{\delta}_2 - \bar{\delta}_3$	4127.616	6	IV	—
4248.224	5	IV	—	4118.555	6	IV	—
4247.440		III	—	4109.810	6	IV	—
4246.089	7?	V	—	4107.499	6	III	—
4245.258		III	—	4100.745	7	IIA	$\bar{F}_5^1 - \bar{F}_4^0$
4238.828	5	IV	—	4098.189	7	IV	—
4235.953	3	III	$\bar{\delta}_4 - \bar{\delta}_4$	4095.980	7	IV	—
4233.614	3	III	$\bar{\delta}_1 - \bar{\delta}_2$	4085.313	5	IV	—
4222.225	6	III	$\bar{\delta}_3 - \bar{\delta}_3$	4085.012		IV	—
4219.364	6	IV	—	4084.508	IV	—	
4216.185	6	I	$d_4^1 - \pi_4$	4071.748	2	II	$F_2^1 - F_2^1$
4210.362	6	III	$\bar{\delta}_1 - \bar{\delta}_1$	4063.604	2	II	$F_3^1 - F_3^1$
4202.032	3	I	$\bar{F}_4^1 - \bar{G}_4^1$	4045.822	2?	II	$\bar{F}_4^1 - \bar{F}_4^1$
4199.093	4	III	—	4040.646	4	V	—
4198.314		III	$\bar{\delta}_5 - \bar{\delta}_4$				
4195.342	6	IV	—	4005.250	6?	II	$\bar{F}_3^1 - \bar{F}_2^1$
4191.446	3	III	$\bar{\delta}_2 - \bar{\delta}_1$	3969.263	4?	II	$\bar{F}_4^1 - \bar{F}_3^1$
4187.812	3	III	$\bar{\delta}_4 - \bar{\delta}_3$	3930.304	4?	I	$d_2^1 - \bar{d}_3^1$
4187.052		III	$\bar{\delta}_3 - \bar{\delta}_2$	3927.925		I	$d_1^1 - \bar{d}_2^1$
4184.894	6	III	—	3922.917	4?	I	$d_3^1 - \bar{d}_1^1$
4181.759	6	III	—	3920.261		I	$d_0^1 - \bar{d}_1^1$
4177.598	6	IIA	$\bar{F}_4^1 - \bar{F}_4^0$	3899.711	4?	I	$d_2^1 - \bar{d}_2^1$
4176.567		IV	—	3898.013		II	$\bar{F}_1^1 - \bar{d}_2^2$
4175.640	6	III	—	3895.659	3	I	$d_1^1 - \bar{d}_0^1$
4174.916		IIA	$\bar{F}_4^1 - \bar{D}_3^0$	3888.520		II	$\bar{F}_2^1 - \bar{D}_2^1$
4172.748	6	IIA	$\bar{F}_1^3 - \bar{D}_2^0$	3887.053	3	I	$\bar{F}_4^1 - \bar{d}_4^2$
4172.128		IV	—	3886.287		I	$d_3^1 - \bar{d}_3^1$
4170.906	6	IV	—	3878.578	3	II	$d_2^1 - \bar{d}_1^1$
4156.805		III	—	3878.024		II	$\bar{F}_3^1 - \bar{d}_3^2$

$\lambda$	Absorption stages	Temperature classes	Notation	$\lambda$	Absorption stages	Temperature classes	Notation
3859.913	3	I	$d_4^1 - \bar{d}_4^1$	3649.308	1	IA	$d_4^1 - f_3^1$
3856.373		IA	$d_3^1 - \bar{d}_2^1$	3647.845		I	I
3850.820	3	II	$\bar{f}_2^1 - p_2^1$	3631.464	1	I	$\bar{f}_3^1 - \bar{g}_4^1$
3849.970		II	$\bar{f}_1^1 - \bar{d}_0^2$	3618.769		2	I
3814.052	3	II	$\bar{F}_2^1 - D_1^1$	3608.860	2	I	$\bar{f}_1^1 - \bar{g}_2^1$
3840.443		II	$f_2^1 - \bar{d}_1^2$	3589.105		?	III
3834.227	3	II	$\bar{f}_3^1 - \bar{d}_2^2$	3586.989	2	II	$\bar{f}_2^1 - \bar{g}_2^1$
3827.826	II	$\bar{F}_3^1 - D_2^1$	3585.708	II		II	$\bar{f}_4^1 - \bar{g}_4^1$
3825.886	3	II	$\bar{f}_4^1 - \bar{d}_3^2$	3585.322	2	II	$\bar{f}_3^1 - \bar{g}_3^1$
3824.444		IA	$d_4^1 - \bar{d}_3^1$	3581.197		2	II
3820.430	3	II	$\bar{f}_5^1 - \bar{d}_4^2$	3570.102	2	II	$\bar{f}_4^1 - \bar{G}_5^1$
3815.844	3	II	$\bar{F}_4^1 - D_3^1$	3565.383	2	I?	$\bar{f}_3^1 - \bar{G}_4^1$
3812.966		II	$\bar{f}_3^1 - P_2^1$	3558.522		3	II
3799.548	4	II	$\bar{f}_3^1 - f_4^2$	3554.121	3	IIIA	$\bar{f}_3^1 - \bar{g}_2^1$
3798.512		II	$\bar{f}_4^1 - f_5^2$	3540.714		3	IIIA
3795.004	4	II	$\bar{f}_2^1 - f_3^2$	3526.167	3	II	$\bar{f}_3^1 - \bar{G}_3^1$
3787.880		II	$\bar{f}_1^1 - f_2^2$	3526.069		3	I
3767.194	3	II	$\bar{f}_1^1 - f_1^2$	3521.264	3	II	$\bar{f}_4^1 - \bar{G}_4^1$
3763.792		II	$\bar{f}_2^1 - f_2^2$	3513.822		3	II
3758.234	3	II	$\bar{f}_3^1 - f_3^2$	3497.842	3	I	$d_1^1 - p_2^1$
3749.487		II	$\bar{f}_4^1 - f_4^2$	3490.577		3	I
3748.264	1	IA	$d_1^1 - f_2^1$	3476.705	3	I	$d_0^1 - p_1^1$
3745.900		IA	$d_0^1 - f_1^1$	3475.454		3	I
3745.563	1	I	$d_2^1 - f_3^1$	3465.864	3	I	$d_1^1 - p_1^1$
3743.336		IIA	$\bar{f}_2^1 - f_1^2$	3443.883		3	I
3737.135	1	I	$d_3^1 - f_4^1$	3440.992	3?	I	$d_3^1 - p_2^1$
3734.869		II	$\bar{f}_5^1 - f_5^2$	3440.614		1	I
3733.319	3	IA	$\bar{d}_1^1 - f_1^1$	3428.200	4	III	—
3727.622		II	$\bar{f}_3^1 - f_2^2$	3424.127		4	III
3722.565	1	IA	$d_2^1 - f_2^1$	3418.514	5	III	—
3719.938		I	$d_4^1 - f_5^1$	3417.847		5	III
3709.250	3	II	$\bar{f}_4^1 - f_3^2$	3413.140	4	III	—
3707.828		I	$d_2^1 - f_1^1$	3407.467		4	III
3705.567	3	I	$d_3^1 - f_3^1$	3306.358	4	III	$\bar{p}_1 - X_2$
3687.458		I	$f_5^1 - \bar{f}_4^2$	3305.980		4	III
3683.056	3	IA	$d_3^1 - f_2^1$	3298.137	6	IV	—
3682.235		IV	—	3292.599		4	IV
3679.915	3	IA	$d_4^1 - f_4^1$				

$\lambda$	Absorption stages	Temperature classes	Notation	$\lambda$	Absorption stages	Temperature classes	Notation	
3286.763	4	III	$\bar{P}_3 - X_3$	2994.50	I	—	$d_3^1 - \bar{d}_2^2$	
3284.593		IV	$\bar{P}_2 - X_2$	2994.434		I	I	$d_0^1 - P_1^1$
3280.268		IV	—	2987.293		2	III	$\bar{F}_4^1 - f_3^3$
3271.013	4	III	$\bar{P}_2 - X_1$	2986.460	2	III	$d_1^1 - P_1^1$	
3265.622	3	III	$\bar{P}_3 - X_2$	2983.571		I	I	$d_4^1 - \bar{d}_3^2$
3265.056		III	$d_2^1 - \bar{D}_3^0$	2981.448	I	I	$d_3^1 - P_2^1$	
3250	3	Most of the lines in this range are reversed, containing those belonging to (d-F) and (d-D).		2973.236	I	I	$d_3^1 - f_4^2$	
~				2973.137		I	I	$d_2^1 - f_3^2$
3100				2970.102		I	I	$\left\{ \begin{array}{l} d_1^1 - f_2^2 \\ d_2^1 - P_1^1 \end{array} \right.$
3100.668	I	II	$\bar{f}_2^1 - \bar{d}_2^3$	2966.902	I	II	$d_4^1 - f_5^2$	
3100.305		II	$\bar{f}_3^1 - \bar{d}_3^3$	2965.258	I?	II	$d_0^1 - f_1^2$	
3099.968	I	II	$\bar{f}_4^1 - \bar{d}_4^3$	2959.996	3	IV	—	
3099.898		II	$\bar{f}_1^1 - \bar{d}_1^3$	2957.370	I?	II	$d_1^1 - f_2^2$	
3091.581	3	II	$\bar{f}_2^1 - \bar{d}_2^3$	2953.943	I?	II	$d_2^1 - f_2^2$	
3083.745	3	II	$\bar{f}_3^1 - \bar{d}_3^3$	2947.876	I?	I	$d_3^1 - f_3^2$	
3075.725	3	II	$\bar{f}_4^1 - \bar{d}_4^3$	2941.343	I?	I	$d_2^1 - f_1^2$	
3067.250	3	II	$\bar{f}_1^1 - \bar{d}_1^3$	2936.903	I	I	$d_4^1 - f_4^2$	
3059.090	I	I	$d_3^1 - \bar{d}_4^2$	2929.006	3	I	$d_3^1 - f_2^2$	
3057.451	3	II	$\bar{f}_5^1 - \bar{d}_4^3$	2926.584	6	IV	—	
3047.608	I	I	$d_2^1 - \bar{d}_3^2$	2923.852		IV	—	
3042.672	I	III	$\bar{f}_2^1 - f_3^3$	2923.289	3	IV	—	
3042.025		III	$\bar{f}_1^1 - f_2^3$	2920.693	6	IV	—	
3041.745		III	$\bar{f}_3^1 - f_4^3$	2918.027	3	IV	—	
3040.430	I	III	$\bar{f}_4^1 - f_5^3$	2912.161	3	I	$d_4^1 - f_3^2$	
3037.392		I	I	$d_1^1 - \bar{d}_2^2$	2901.919	6	IV	—
3031.641	3	III	$\bar{f}_1^1 - f_1^3$	2901.384	IV		—	
3026.468	I	III	$\bar{f}_2^1 - f_2^3$	2899.418	6	IV	—	
3025.846		I	I	$d_0^1 - \bar{d}_1^2$	2895.036	3	III	$\bar{F}_3^1 - Z_3$
3024.035	I	IA	$d_1^1 - P_2^1$	2894.506	3	III	—	
3021.076		I	$d_3^1 - \bar{d}_3^2$	2883.726?		3	V	—
3020.643		I	I	$d_4^1 - \bar{d}_4^2$		2877.363	3?	III
3020.495	I	II	$d_2^1 - \bar{d}_3^2$	2874.176	3	I	$d_4^1 - \bar{g}_5^1$	
3009.575		II	$\bar{f}_4^1 - f_4^3$	2869.313	3	I	$d_3^1 - \bar{g}_4^1$	
3008.142	I	I	$d_1^1 - \bar{d}_0^2$	2863.866	3	I	$d_2^1 - \bar{g}_3^1$	
3007.284		I	I	$d_2^1 - P_2^1$	2851.798	I	II	$\bar{f}_1^1 - \bar{g}_2^2$
3000.951	I	I	$d_2^1 - \bar{d}_1^2$					
2999.516		II	$\bar{f}_5^1 - f_5^3$					

$\lambda$	Absorption stages	Temperature classes	Notation	$\lambda$	Absorption stages	Temperature classes	Notation	
2843.974	I	II	$\bar{f}_2^1 - \bar{g}_3^2?$	2739.551	3	—	—	
2843.928		II	$d_2^1 - \bar{g}_2^1$	2737.312	I	II	$d_1^1 - p_1^2$	
2843.629		III	$\bar{f}_4^1 - p_3^3$	2736.970		—	—	
2840.422		6	II	$d_3^1 - \bar{g}_3^1$	2735.480	I	III	—
2838.118		3	II	$f_2^1 - \bar{g}_2^2?$	2733.580	I	II	—
2835.455		6	I	$d_4^1 - \bar{g}_4^1$	2723.582	I	II	$d_2^1 - p_1^2$
2832.433		I	II	$f_3^1 - \bar{g}_4^2?$	2720.910	I	II	$d_3^1 - p_2^2$
2825.687		I	II	$d_4^1 - \bar{f}_5^1$	2719.037	I	II	$d_4^1 - p_3^2$
2825.556			II	—	2714.419	3	—	—
2823.276		I	II	$\bar{f}_3^1 - \bar{g}_3^2?$	2711.848	3	III	—
2813.288	3	II	$\bar{f}_4^1 - \bar{g}_5^2?$	2711.662	III		—	
2807.244	3	III	$d_4^1 - \bar{g}_3^1$	2708.580	3	IV	—	
2806.985		II	—	2706.590	3	III	—	
2804.523	3	III	$\bar{f}_5^1 - \bar{g}_5^2?$	2699.114	3	III	—	
2801	Mn?	—	—	2696.290	I	—	—	
2798		—	—	2695.998		—	—	
2795		—	—	2689.220	2	III	—	
2788.108		I 2	II	—	2679.066	3	—	—
2787.938			II	—	2667.918	—	IIIA	$d_2^1 - D_3^1$
2781.804		3	III	—	2666.970	3	III	—
2778.226		3	III	$\bar{f}_5^1 - \bar{g}_5^2?$	2666.818	—	IIIA	—
2772.112		I	III	$d_2^1 - p_3^2$	2662.066	3	III	—
2767.618		3	III	—	2656.154	2	III	—
2762.029		3	III	—	2647.568	2	III	$d_3^1 - D_3^1$
2761.788	III		—	2644.008	2	III	—	
2756.332	I	I	$d_1^1 - p_2^2$	2641.654	2	III	—	
2756.270		—	$d_3^1 - \bar{f}_4^1$	2636.489	2	III	—	
2755.736		—	—	2635.818		III	—	
2754.428		—	III	—	2631.332	2	—	—
2754.032	I	III	—	2631.053	—	—	—	
2753.688	—	III	—	2628.303	3	—	—	
2750.145	I	II	$d_3^1 - p_3^2$	2625.676	3	—	—	
2746.998	3	—	—	2623.544	2	III	—	
2746.486		III	—	2621.677	6	—	—	
2744.072	I	II	—	2617.627	2	—	—	
2742.408	I	II	$d_2^1 - p_2^2$	2613.835	2	—	—	
2742.021		III	$d_2^1 - \bar{f}_3^1$	2611.885	3	—	—	

$\lambda$	Absorption stages	Temperature classes	Notation	$\lambda$	Absorption stages	Temperature classes	Notation
2607.099	2	—	—	2488.148	I	II	$d_3^1 - f_4^3$
2606.839		III	—	2484.188	I	II	$d_1^1 - f_1^3$
2605.687	6	III	—	2483.277		I	II
2599.577	I	III	—	2479.782	I	II	$d_2^1 - f_2^3$
2599.405		—	—	2476.68	2	III	—
2598.380	2	—	—	2474.818	2	—	—
2594.161	2	III	—	2472.910	I	II	$d_3^1 - f_3^3$
2594.064		III	—	2472.875		—	—
2592.796	4	—	—	2472.351	—	III	—
2591.554		—	—	2465.155	I	III	—
2588.010	3	III	—	2462.652	I	II	$d_4^1 - f_4^3$
2585.886	4	IV	—	2462.191		III	$d_3^1 - f_2^3$
2584.544	I	—	—	2457.602	2	II	—
2582.590	3	—	—	2453.478	2	III	—
2582.310		III	—	2447.714	2	II	$d_4^1 - f_3^3$
2576.111	I	—	—	2442.574	2	—	—
2566.920	3	—	—	2439.740	2	—	—
2563.485	3	—	—	2438.19	2	III	—
2562.543		—	—	2413.313	3	—	—
2549.616	I	III	$d_3^1 - \bar{d}_4^3$	2411.071	3	—	—
2545.979	I	III	$d_2^1 - \bar{d}_4^3$	2410.526		—	—
2544.716 ?	2	IV	—	2406.663	3	—	—
2543.927 ?	I	IV	—	2404.888	I	—	—
2542.105	2	—	—	2404.435		—	—
2540.976	I	III	$d_1^1 - \bar{d}_2^3$	2399.244	3	—	—
2535.610	I ?	III	$d_0^1 - \bar{d}_1^3$	2395.628	I	—	—
2529.832	I	III	$d_1^1 - \bar{d}_1^3$	2395.423		—	—
2529.137		III	$d_1^1 - \bar{d}_2^3$	2389.979	2	—	$d_2^1 - p_3^3$
2527.44	I	II	$d_3^1 - \bar{d}_3^3$	2388.631	2	—	—
2524.291	I	II	$d_1^1 - \bar{d}_0^3$	2382.039	I	II	—
2522.855	I	II	$d_4^1 - \bar{d}_4^3$	2381.85		—	—
2518.107	I	II	$d_3^1 - \bar{d}_1^3$	2380.763	3	—	—
2510.837	I	II	$d_3^1 - \bar{d}_2^3$	2379.276		—	—
2501.135	I	II	$d_4^1 - \bar{d}_3^3$	2375.193	4	—	—
2491.162	I	II	$d_1^1 - f_2^3$	2373.733	2	—	—
2490.659		II	$d_2^1 - f_3^3$	2373.624		—	—
2489.759	II	$d_0^1 - f_1^3$	2370.49	3	—	—	





The number added to the vertical line, which represents absorption, approximately indicates the stage, in which the multiplet came out reversed in my spectrograms.

It is to be observed from the diagram that:

(1) The absorption that starts from the higher level generally occurs in the later stages, as ought to be expected.

(2) For the multiplets that have a common lower level, that for which the upper level is higher seems to be reversed in the earlier stages. (The order is just reversed for copper, as will be seen from Fig. c. Why such should be the case is unknown at present. In consideration of the complicating factors (enumerated in Note I) that come into play in the determination of stages, the case is not simple and more detailed and elaborate study seems necessary.)

As to the order of reversal of the lines within a multiplet, the lines belonging to ( $\bar{F}^1 - \bar{g}^1$ ) may be taken as a typical example.

Thus:

	$\lambda$	(Stage)	(intensity)
$\bar{F}_4^1 - \bar{g}_5^1$	(4384)	2	45
$F_3^1 - \bar{g}_4^1$	(4405)	3	30
$\bar{F}_2^1 - \bar{g}_3^1$	(4415)	4	20
$\bar{F}_4^1 - \bar{g}_4^1$	(4294)	5	15
$\bar{F}_3^1 - \bar{g}_3^1$	(4337)	5	10
$F_2^1 - \bar{g}_2^1$	(4368)	no absorp.	2
$F_4^1 - \bar{g}_3^1$	(4230)	no absorp.	1
$\bar{F}_3^1 - \bar{g}_2^1$	(4291)	no absorp.	4

The lines that are stronger in emission are more easily reversed. The same seems to hold for all other multiplets.

The impurity iron lines that were identified in the spectrograms of copper (Fig. B) and mercury (Figs. A and C) are given in the following:

4415	$\bar{F}_2^1 - \bar{g}_3^1$	4326	$\bar{F}_2^1 - \bar{G}_3^1$	} (Fig. B)
4405	$\bar{F}_3^1 - \bar{g}_4^1$	4308	$\bar{F}_3^1 - \bar{G}_4^1$	
4384	$\bar{F}_4^1 - \bar{g}_5^1$	4272	$\bar{F}_4^1 - \bar{G}_5^1$	
3959	$d_3^1 - \bar{d}_4^2$	2737.312	$d_1^1 - p_1^2$	}
3048	$d_2^1 - \bar{d}_3^2$	2736.970	—	
3037	$d_1^1 - \bar{d}_2^2$	2734	—	
3026	$d_0^1 - \bar{d}_1^2$	2724	$d_2^1 - p_1^2$	
3021	$d_3^1 - \bar{d}_3^2, d_4^1 - \bar{d}_4^2, d_2^1 - \bar{d}_3^2$	2721	$d_3^1 - p_2^2$	

3008	$d_1^1 - \bar{d}_0^2$	2719	$d_4^1 - p_3^2$	} (Fig. 6 <sub>2</sub> )
3001	$d_2^1 - \bar{d}_1^2$	2550	$d_3^1 - \bar{d}_4^3$	
2995	$d_3^1 - \bar{d}_2^2$	2546	$d_2^1 - \bar{d}_4^3$	
2984	$d_4^1 - \bar{d}_3^2$	2544	—	
2973	$d_3^1 - f_4^2, d_2^1 - f_3^2$	2527	$d_3^1 - d_3^3$	
2967	$d_4^1 - f_5^2$	2523	$d_4^1 - \bar{d}_4^3$	
2750	$d_3^1 - p_3^2$	2518	$d_2^1 - \bar{d}_1^3$	
2744	—	2511	$d_3^1 - d_2^3$	
2742	$d_2^1 - p_2^2$	2501	$d_4^1 - d_3^3$	
2740	—	2491	$d_1^1 - f_2^3, d_2^1 - f_3^3$	
	etc.			

These all belong to the characteristic arc lines.

#### § 4. Summary.

Thus far the explosion spectra have been investigated for mercury, copper, and iron. Prominent results attained are:

(1) Continuous back-ground is satisfactorily developed by the explosion of mercury in a confined space at atmospheric pressure as well as under a reduced pressure.

(2) A good many absorption lines (either series or non-series lines) due to the excited atoms of these elements were obtained.

(3) By varying the voltage at which the explosion occurs, the manner, in which a line came out reversed after another, was studied.

(4) Subordinate series lines of Na, unclassified pairs and triplets of Ca, arc lines of Si, Swan spectrum, etc. were reversed as impurities.

The study of the absorption spectra produced by the explosion is to be continued for other elements.

In conclusion; the writer wishes to express his deepest appreciation to Professor M. Kimura, under whose direction this work was done, and to Professor U. Yoshida for the interest he has taken in the work.

Plate I.

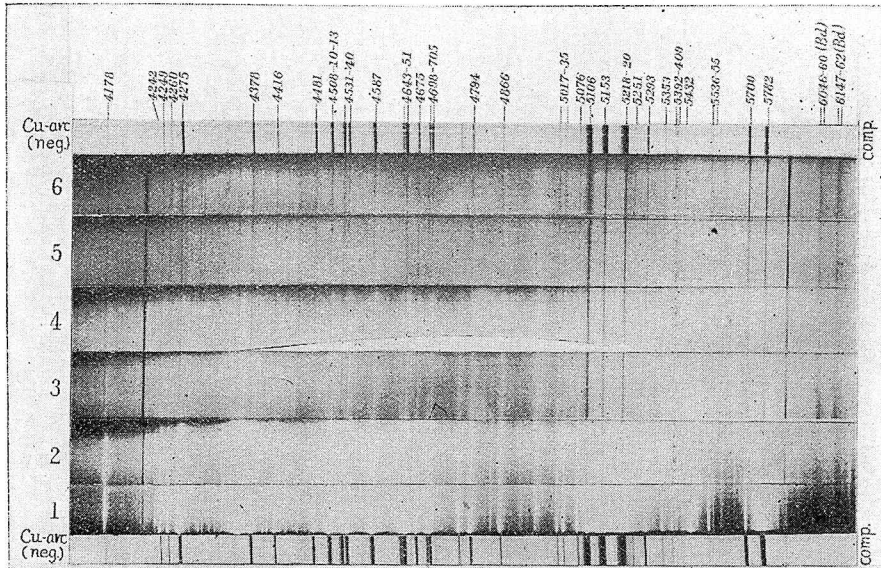


Fig. 1. (Cu)

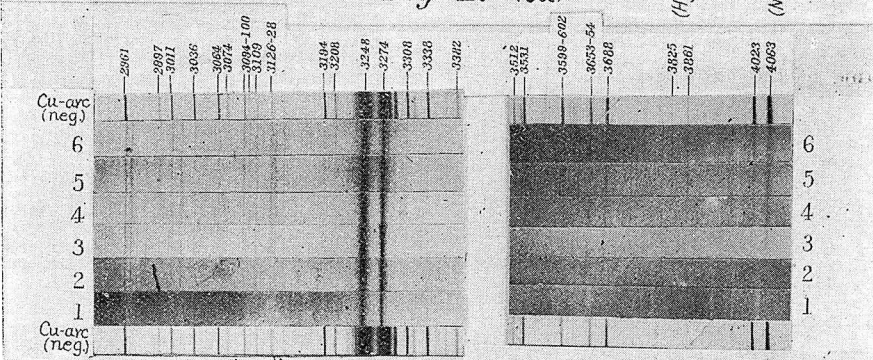


Fig. 2. (Cu)

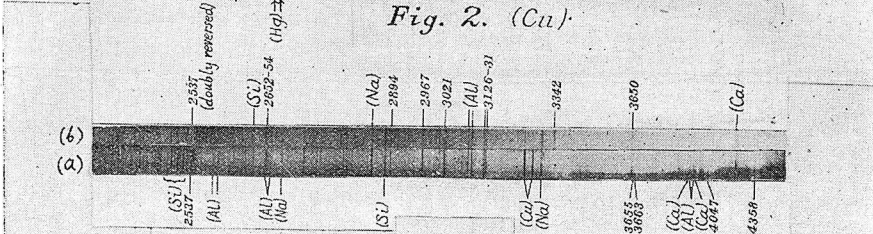


Fig. A. (Cu)

(a) Explosion in air; (b) Explosion under reduced press.

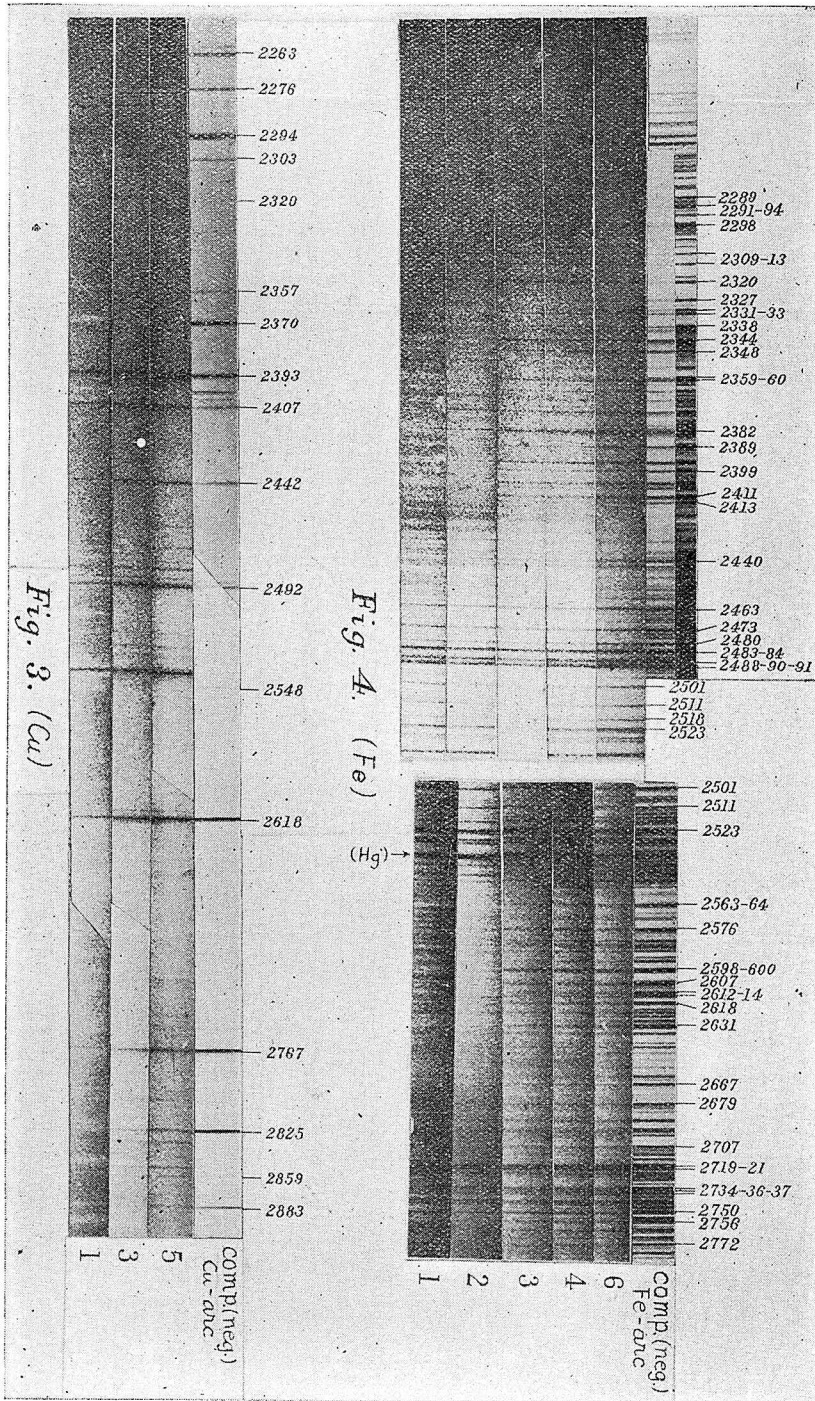


Plate IV.

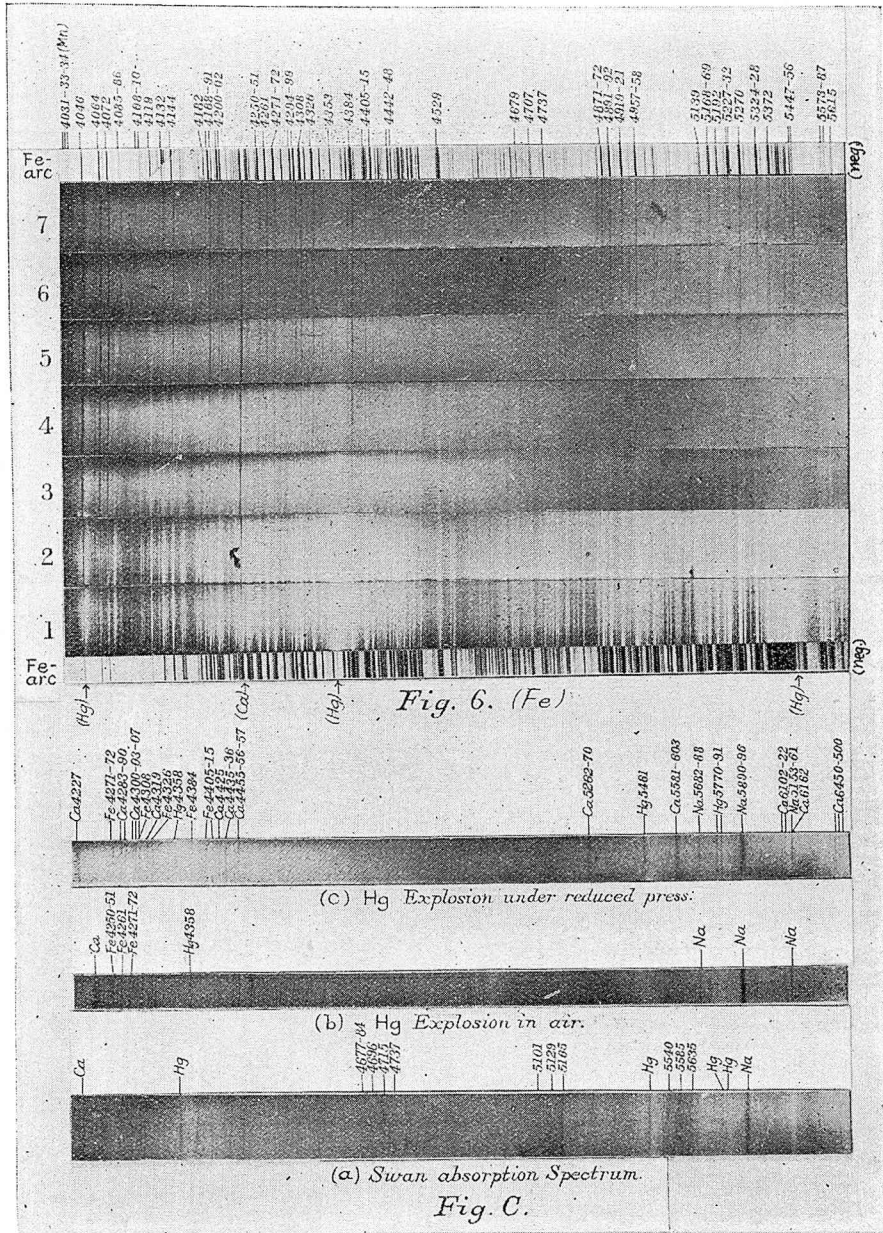


Plate III.

